Numerical study of the reflected elastic waves using Rayleigh diffraction integral

Nadir Maghlaoui, Hakim Djelouah, Assia Oudina, Mohamed Ourak, Farouk Benmeddour

Numerical study of the reflected elastic waves using Rayleigh diffraction integral

IOP Conf. Series: Materials Science and Engineering **657** (2019) 012014 doi:10.1088/1757-899X/657/1/012014

Numerical study of the reflected elastic waves using Rayleigh diffraction integral

N Maghlaoui[1,4], H Djelouah[2], A Oudina [2], M Ourak[3] and F Benmeddour[3]

[1]Ecole Supérieure en Sciences Appliquées d'Alger, BP 474, Place des Martyrs 16001, Alger, Algérie
[2]Université des Sciences et de la Technologie Houari Boumediene, Faculté de Physique, Laboratoire de Physique des Matériaux, BP 32 El Alia 16111, Algiers, Algeria
[3]Univ. Polytechnique Hauts-de-France, CNRS, Univ. Lille, YNCREA,Centrale Lille, UMR 8520 - IEMN, DOAE, F-59313 Valenciennes, France

E-mail : maghlaoui.n79@gmail.com

Abstract. In this work, the transient ultrasonic waves radiated by a linear phased array transducer in a liquid then reflected at a liquid solid interface is studied. A model based on the Rayleigh integral is used where the reflection at the plane interface is considered by using the reflection coefficients for harmonic plane waves. The transient field is obtained by an inverse Fourier transform of the harmonic field. The obtained results highlight the different components of the ultrasonic field: the direct and edge waves as well as the longitudinal head waves or leaky Rayleigh waves. The temporal representation of these waves has been analyzed and discussed by the rays' model. Instantaneous cartographies allowed a clear description of all the waves which appear at the liquid-solid interface. The results have been compared to those obtained by using a finite element method.

1. Introduction

The propagation study of the ultrasonic waves at the interface liquid solid radiated by a multi-element linear transducer has been the subject of many publications [1-9].
The advantage of multi-element transducers is to allow the focusing and the steering of the beam in both liquid and solid [1- 10].

Generated acoustic waves by elementary sources composing a transducer can be modeling by superposing the produced fields. Each source is modeled by point source superposition applied to the Rayleigh integral, the spatial impulse response model, and other analytically equivalent integral approaches.

A good review of the earlier developments of the acoustic wave modeling generated by multi-element linear transducers in front of a planar liquid solid interface can be found in [8, 11-21].
In this research work, the Rayleigh integral has been used to simulate the propagation of the ultrasonic wave emitted in water by a multi-element linear transducer in presence of a plane water-solid interface. This model starts from the knowledge of the particle velocity at the radiating surface. Then, the harmonic velocity potential is derived through the Rayleigh integral on the surface. The transient incident wave is then obtained by an inverse time Fourier transform of the harmonic results. In the presence of a fluid solid interface the echo-graphic response in the liquid is calculated by taking into

account the reflection coefficient for harmonic plane waves. The obtained results highlighted the different components of the acoustic field in the liquid: the bulk waves as well as the surface waves radiated in the water. The temporal representation of these waveforms has been studied. The arrival time of each contribution is analytically calculated and the physical origin of each of them is clearly determined (Table 1). Time domain snapshot of different wave front propagation before and after reflection allowed a physical description of all waves. These results are compared with those obtained by a finite element method [22].

2. Theoretical model

2.1. Analytical formulation

2.1.1. Emission in the water

A multi-element linear transducer comprising *N* small sources is considered. The latter emits acoustic waves in water, the propagation velocity of these waves is c_f. The width of each source is $2a$ and the distance between the center of two successive source is denoted d. Let $\mathcal{R}(\overrightarrow{Ox}, \overrightarrow{Oz})$ be the reference frame where $\overrightarrow{Ox}$ is taken as the reference line defining the z = 0 plane and the second axis $\overrightarrow{Oz}$ perpendicular to the previous axis (figure 1).

Assuming that the radiating surface is a set of elementary sources and each elementary surface *dS* vibrates with a uniform normal particle velocity $v_n(t)$.

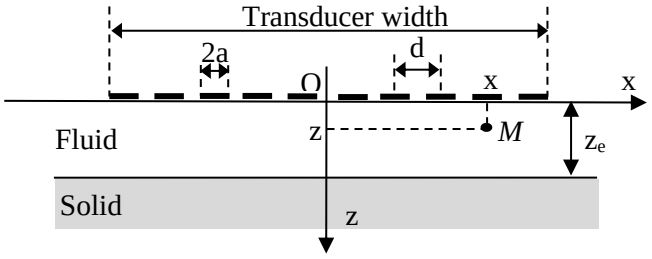

Figure 1. Geometry of the problem

At a point $M(x,z)$ in a water, the pressure $p_j(x,z,t)$ radiated by the j[th] element of the multi-element source can be expressed is:

$$p_j(x,z,t) = \rho_f \frac{\mathrm{d}\varphi_j(\mathrm{x},z,t)}{\mathrm{dt}}, \tag{1}$$

$\varphi_j(\mathrm{x},z,t)$ is the transient velocity potential at the field point (x,z).

$$\bar{\varphi}_j^*(k_x,z,\omega) = \int_{-\infty}^{+\infty} \varphi_j^*(x,z,\omega)\, exp(-ik_x x)\, dx. \tag{2}$$

Equation (2) shows that the velocity potential $\varphi_j(x,z,t)$ at any point inside the medium is a harmonic synthesis of monochromatic plane waves $\bar{\varphi}_j^*(k_x,z,\omega)$.

$\bar{\varphi}_j^*(k_x,z,\omega)$ is the spatial Fourier transform of the velocity potential $\varphi_j^*(x,z,\omega)$ calculated in the monochromatic case by the Rayleigh integral:

$$\varphi_j^*(x,z,\omega) = \frac{v_{nj}^*(\omega)}{2\pi} \iint_S \frac{exp(ikr)}{\sqrt{r}}\, dS, \tag{3}$$

where dS is the array of the elementary sources constituting the j[th] element, r is the distance from the point $M(x,z)$ to the elementary source, $k = \omega/c_f$ is the wave number, ω is the angular frequency. Each transducer element is constituted from elementary sources which vibrate with a velocity $v_{nj}(x,t)$.

$$v_{nj}^*(\omega) = \int_{-\infty}^{+\infty} v_n\left(t-\tau_j\right) exp(i\omega t)\, dt, \tag{4}$$

where $v_{nj}(x,t)$ and τ_j are respectively the particle velocity and the time delay associated with the j[th] element of the transducer.

The wave field at the point $M(x,z)$ is the sum of the wave fields emitted by the *N* elements of the multi-element transducer:

$$p(x,z,t) = \sum_{j=1}^{N} p_j(x,z,t) \tag{5}$$

In order to obtain a focusing beam, the time delay applied to the j[th] element is:

$$\tau_j = \frac{F - \sqrt{(x_f - x_j)^2 + z_f^2}}{c_f} \tag{6}$$

where $F(x_f, z_f)$ is the focal point.

2.1.2. Water and aluminium media separated by a plane interface

In the presence of the water aluminium plane interface at $z = z_e$. The incident wave at the interface defined by $z = z_e$ plane, is given by:

$$p_i(x,z_e,t) = \sum_{j=1}^{N} p_{ij}(x,z_e,t), \tag{7}$$

with

$$p_{ij}(x,z_e,t) = \rho_f \frac{d\varphi_{ij}(x,z_e,t)}{dt}, \tag{8}$$

where φ_{ij} is the incident velocity potential radiated by the j[th] element of the source.

The space time Fourier transform of the velocity potential radiated by the j[th] element of the source and reflected at the interface is:

$$\bar{\varphi}^*_{rj}(k_x,z_e,\omega) = \bar{\varphi}^*_{ij}(k_x,z_e,\omega)\boldsymbol{R}(k_x,\omega), \tag{9}$$

where $\boldsymbol{R}(k_x,\omega)$ is the reflection coefficient at the water-aluminium plane interface.

The reflection coefficient $\boldsymbol{R}(k_x,\omega)$ is calculated by taking into account the specular and non specular reflection. Considering the fact that the reflected pressure must be real valued functions, their Fourier transforms must be Hermitian.

The echo-graphic response of the wave coming back to a z-plane is given by:

$$p_r(x,z,t) = \sum_{j=1}^{N} p_{rj}(x,z,t), \tag{10}$$

where

$$p_{rj}(x,z,t) = \rho_f \frac{d\varphi_{rj}(x,z,t)}{dt}, \tag{11}$$

$p_{rj}(x, z, t)$ is the echo-graphic response of the pressure field emitted by the j[th] source.

2.2. Numerical implementation

MATLAB programs have been developed to model the acoustic field in presence of a water-aluminium interface using Rayleigh integral method.

The waveform over the active surface of the source is represented by the excitation signal *f*(*t*), (figure 2), which is a pulse whose center frequency is f =1 MHz defined by:

$$f(t) = A\cos[2\pi f(t-t_0)]\exp\{-(t-t_0)^2/B\}. \tag{12}$$

The propagation medium is water, characterized by an acoustic velocity c_f = 1485 ms^{-1} and whose density is $\rho_f = 10^3 \mathrm{kg/m^3}$. The solid is aluminum for which the velocities of the longitudinal and transverse waves are respectively: c_L = 6420 ms^{-1}, c_T = 3110 ms^{-1} and whose density is $\rho_s = 2.7 \cdot 10^3 \mathrm{kg/m^3}$.

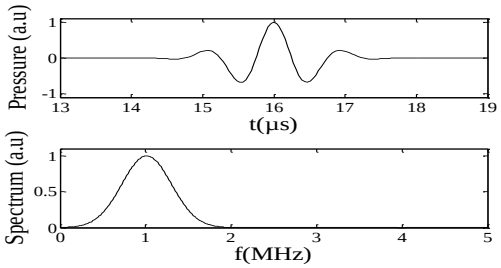

Figure 2. Time waveform $p(0,t)$ and its time Fourier transform. Frequency f = 1 MHz, B = 5 10^{-13} s^2 and $t_0 = 16$ μs.

3. Discussion

3.1. Obtained results

In order to explain the different kind of contribution to the echo-graphic response, the characteristics of the wave emitted by a cylindrical transducer [8] is used. The field emitted forward by the source is the superposition of two contributions: the direct wave emanating from the front face of the source and the edge waves from the edge of the source. When these contributions arrive at the solid surface, they are reflected and transmitted (figure A1 – A2).

Considering that, during the propagating time, the circular edge waves sweep over the solid surface. The reflection phenomenon can be described by simply considering an incident wave emerging from the edge of the multi-element source and having an incidence angle varying with time.

Figure 3 (a) represents the pressure received by the 64th element of multi-element transducer, located at the middle of the phased array transducer. In this case the first impulse corresponds to the superposition between the reflected direct wave and the longitudinal head wave followed by the superposition between the leaky Rayleigh wave (RW) and the reflected edge waves (REW). In this case the reflected direct wave is due to the reflection of the direct wave by the aluminum surface, which arrives to the 64th element of phased array transducer. The leaky Rayleigh wave (RW) is due to the conversion of the direct wave, incident at Rayleigh incidence angle ($\theta = 30.65°$), into a surface wave which propagates at the velocity $c_R = 2917\ \mathrm{ms}^{-1}$ over the solid surface.

Figure 3 (b) represents the reflected wave, received by the elements from 62th to 66th of phased array transducer. This signal is obtained by a simple summation of the received pressure by the elements 62th to 66th. The first wave corresponds to the interference between the reflected direct wave and the longitudinal head wave. The next wave corresponds to the interference between the leaky Rayleigh wave (RW) and the reflected edge waves (REW). It is worth noting that the amplitude of the reflected direct wave (RDW) is significant compared to the other contributions (REW, RW and LW).

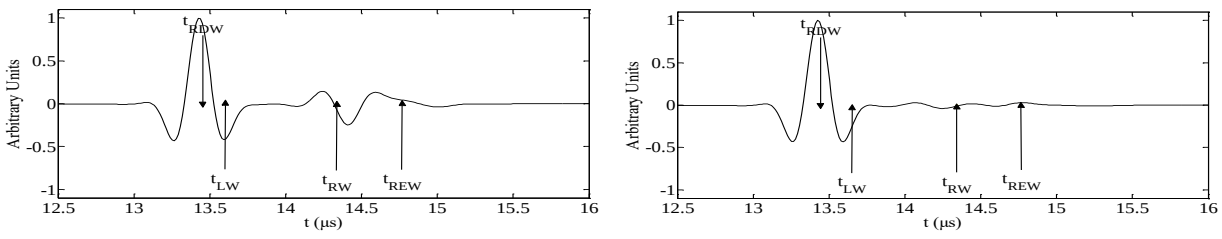

(a) (b)

Figure 3. Representation of the wave (Arbitrary units) received by the transducer. Number of

elements N = 128, Width $2\ a$ = 0.27 mm, pitch of the elements d = *0.3 mm*, f = 2.5 MHz, plane interface z_e = 10 mm, Focal point $F(x_f = 0, z_f = 30mm)$. (a) Wave field received by the 64th element of the multi-element source, (b) Wave field received by the elements from 62 to 66 of the multi-element source.

Figure 4 represents the pressure wave fronts at different instant times. At the time t = 2.68 μs (figure 4 (a)) the presence of the longitudinal bulk waves (DW and EW) is observed. The different wave fronts are focused on the field point $F(x = 0\ mm, z = 20\ mm)$ from the multi-element source. After reflection, $t = 12.19\ \mu s$ (figure 4 (b)), the presence of the wave front (RDW) and the wave fronts (REW) are noticed. These waves are due to the specular reflection of the direct and edge waves at water solid interface. It is also noted the presence of weak amplitude waves identified by the leaky Rayleigh wave (RW) and the longitudinal head wave (LW) (figure 4 (b)). These waves are characterized by a linear wave front propagating in the direction $\theta = \pm 30.65°$ in the case of the Rayleigh wave (RW) and in the direction $\theta = \pm 13.39°$ in the case of the longitudinal head wave (LW). Inside the radiated zone, the non-specular contributions are due to the non-specular reflection of the direct wave arriving onto the interface with critical incidence angles. Outside the radiated zone, the non-specular contributions are due to the non-specular reflection of the edge wave arriving onto the interface with critical incidence angles. Furthermore, the energy converted to the longitudinal head wave is weaker than that converted to the leaky Rayleigh wave.

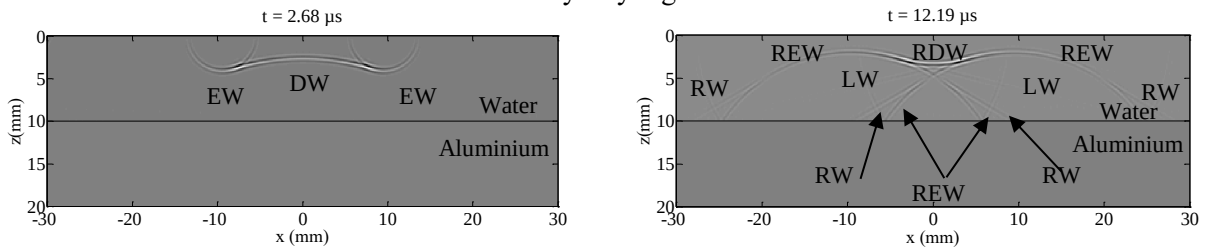

(a) (b)

Figures 4. Representation of the wave field $p(x, z)$ before and after reflection by the water aluminium interface. Transducer parameter (N = 128, $2a$ = 0.13 mm, d = *0.15 mm*, f = 2.5 MHz), z_e = 10 mm, $F(x_f = 0, z_f = 30\ mm)$. (a) Before reflection t = 2.68 µs, (b) After reflection t = 12.19 µs.

3.2. Comparison with finite element method

Finite element method has been used for comparison purposes by using a finite element package [8, 22 - 23].

The choice of the finite element method mesh must be able to reproduce the propagation and the reflection of the elastic wave. The spatial and time steps Δx, Δz and Δt verify the conditions:

$$\max(\Delta x, \Delta z) < \lambda_{min}/10 \quad \text{and} \quad \Delta t < 0.7\frac{\min(\Delta x, \Delta z)}{c_L}, \tag{13}$$

where λ_{min} is the smallest wavelength associated to the maximum frequency spectrum. The used time discretization step is $\Delta t = 0.015 \mu s$.

The incident and reflected pressure fields are computed by the finite element model in the presence of the water aluminum plane interface, the obtained results are shown in figure 5. The results put in evidence the bulk waves (Figure 5 (a)). After reflection, at the instant time $t = 13.60\ \mu s$, the different waves are reflected and generate the reflected bulk wave (RDW and REW) and the surface waves which radiate in water (RW and LW).

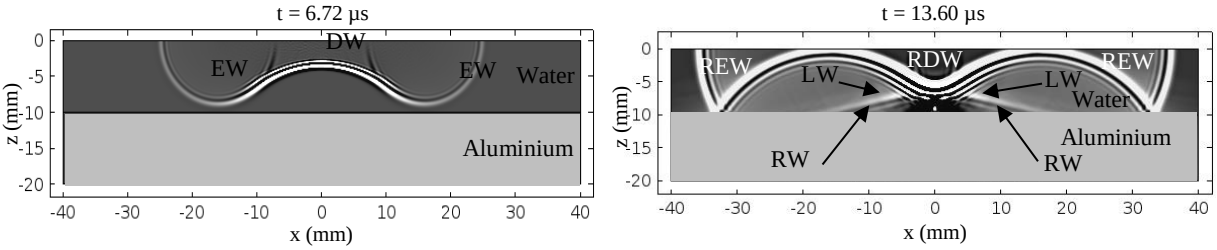

(a) (b)

Figure 5. Representation of the wave field $p(x, z)$ before and after reflection by the water aluminium interface. Transducer parameter (N = 128, $2a$ = 0.2 mm, d = 0.25 mm, f = 2.5 MHz), z_e = 10 mm, $F(x_f = 0, z_f = 20mm)$. (a) Before reflection t = 6.72 µs, (b) After reflection t = 13.60 µs.

These contributions are identified by a linear wave front propagating in the direction $\theta = 13.39°$ in the longitudinal head wave (LW) case and the direction $\theta = 30.65°$ in the leaky Rayleigh (RW) case (Figure 5 (b)).

At the frequency $f = 2.5\ MHz$ and for the element number $N = 128$, the computing time is 691.80 s with the finite element method and 126.20 s with the Rayleigh integral method, respectively in a computer with an Intel Pentium Core (TM) i7 2.4 GHz processor.

4. Conclusion

Rayleigh integral method is used to model the ultrasonic wave generated by multi-element linear transducer in front of the water-aluminum interface. This semi analytical model considers the radiation, the specular and non-specular reflection. One major advantage of this method is to use the expression of the reflection coefficient, which reduces the computing time. One other advantage of the Rayleigh integral method is its capability of modeling critical reflection phenomenon.

The computed results show the advantage provided by the linear array transducer in the acoustic microscopy application.

The obtained results agree with those computed with the finite element method.

The method can be extended to the case of more complex transducers or more complex structure.

Appendix

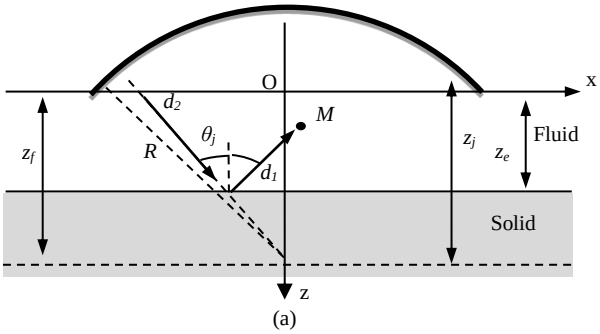

(a)

Figure A1. Paths of the reflected Bulk wave contributions.

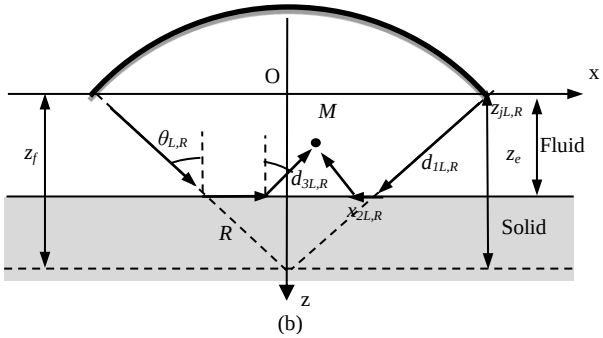

(b)

Figure A2. Paths of the Leaky wave contributions.

Table 1. The calculation of the arrival times of the reflected waves are detailed in [8].

Bulk reflected waves (Figure A1)	Leaky surface waves (Figure A2)
$t_{RDW} = \frac{d_1 + d_2}{c_f}$	$t_{RW} = \left(\frac{d_{1R}}{c_f} + \frac{d_{2R}}{c_f} + \frac{x_R}{c_R}\right)$
$t_{REW} = \left(\frac{\sqrt{(z_e - z)^2 + x_1^2}}{c_f}\right) + \left(\frac{\sqrt{{z_e}^2 + x_2^2}}{c_f}\right)$	$t_{LW} = \frac{d_{1L}}{c_f} + \frac{d_{3L}}{c_f} + \frac{x_{2L}}{c_L}$

References

[1] Frénet D, Calmon P and Ouaftouh M 1998 Generation of leaky Rayleigh waves using a conical phased-array transducer : modeling time-domain signals on anisotropic materials *Proc. IEEE Ultrason. Symp Japan* **1** 269-72
[2] Zeng X and McGough R J 2009 Optimal simulations of ultrasonic fields produced by large thermal therapy arrays using the angular spectrum approach *J. Acoust. Soc. Am.* **125**(5) 2967-77
[3] Wu P, Kazys R and Stepinsky T 1995 Calculation of transient fields in immersed solids radiated by linear focusing arrays *Proc. IEEE Ultrason. Symp.* **2** 993-7
[4] Titov S, Maev R and Bogachenkov A 2006 Measurements of velocity and attenuation of leaky waves using an ultrasonic array *Ultrasonics* **44** 182-7
[5] Banerjee S, Kundu T and Alnuaimi N A 2007 DPSM technique for ultrasonic field modelling near fluid–solid interface *Ultrasonics* **46** 235-50
[6] Ahmad R, Kundu T and Placko D 2005 Modeling of phased array transducers *J. Acoust. Soc. Am.* **117**(4) 1762-76
[7] Banerjee S and Kundu T 2007 Ultrasonic field modeling in plates immersed in fluid *Int. J. Sol. Str.* **44** 6013–29
[8] Maghlaoui N, Belgroune D, Ourak M and Djelouah H 2016 Reflection at a liquid–solid interface of a transient ultrasonic field radiated by a linear phased array transducer *Ultrasonics* **71** 98-105
[9] Belgroune D, de Belleval J F and Djelouah H 2008 A theoretical study of ultrasonic wave transmission through a liquid-solid interface *Ultrasonics* **48** 220-30
[10] Song S J and Kim C H 2002 Simulation of 3-D radiation beam patterns propagated through a planar interface from ultrasonic phased array transducers *Ultrasonics* **40** 519-24
[11] Oberhettinger F 1961 On transient solutions of the baffled piston problem *J. Res. Nat. Bur. Stand.* **65B** 1-6
[12] Stepanishen R P 1971 Transient radiation from piston in an infinite planar baffle *J. Acoust. Soc. A.* **49**(5) 1629-38
[13] Harris G R 1981 Review of transient field theory for a baffled planar piston *J. Acoust. Soc. A.* **70** 10-20
[14] Wu P, Kazys R and Stepinski T 1995 Analysis of the numerically implemented angular spectrum approach based on the evaluation of two-dimensional acoustic fields. Part I. Errors due to the discrete Fourier transform and discretization *J. Acoust. Soc. A.* **99** 1139-48
[15] Lerch T P, Schmerr L W, Sedov A 1998 Ultrasonic beam models: an edge element approach *J. Acoust. Soc. A.* **104**(3) 1256-65
[16] Zhang J, Guy P, Baboux J C and Jayet Y 1999 Theoretical and experimental responses for a large-aperture broadband spherical transducer probing a liquid–solid boundary *J. App. Phy.* **86**(5) 2825-35
[17] Fellinger P, Marklein R, Langenberg K J and Klaholz S 1995 Numerical modeling of elastic wave propagation and scattering with EFIT-elastodynamic finite integration technique *Wave Motion* **21** 47-66
[18] Rappel H, Yousefi-Koma A, Jamali J and Bahari A 2014 Numerical Time-Domain Modeling of Lamb Wave Propagation Using Elastodynamic Finite Integration Technique *Shock Vib.* **2014**(6) 1-6
[19] Zhu J, Popovics J S Schubert F 2004 Leaky Rayleigh and Scholte waves at the fluid–solid interface subjected to transient point loading *J. Acoust. Soc. A.* **116** (4) 2101–10
[20] Wu P, Kazys R and Stepinsky T 1995 Calculation of transient fields in immersed solids radiated by linear focusing arrays *Proc. IEEE. Ultrason. Symp*. **2** 993-7
[21] Du Y, Jensen H, Jensen J A 2013 Investigation of an angular spectrum approach for pulsed ultrasound fields *Ultrasonics* **53** 1185–91
[22] http://www.COMSOL.com

[23] Yuan M, Kang T, Zhang J, Song S J and Kim H J 2013 Numerical simulation of ultrasonic minimum reflection for residual stress evaluation in 2D case *J. Mech. Sci. Technol.* **27**(11) 3207-14